Vulcano Workshop 2006
The Role of Relativistic Jets in Astroparticle Physics

J. H. Beall

E. O. Hulbert Center for Space Research,
Naval Research Laboratory, Washington, DC;
CEOSR/School of Computational Sciences, GMU, Fairfax, VA; and
St. Johns College, Annapolis, MD.

With thanks to my colleagues:

J. Guillory, School of Computational Sciences, George Mason University, Fairfax, VA,
D. V. Rose, Voss Scientific, Albuquerque, NM,
S. Schindler, University of Innsbruck, Innsbruck, Austria, and
S. Colafrancesco, INAF – Osservatorio Astronomico di Roma, Monteporzio, Italy

First, a bit of humor:

What does a physicist says when he or she is asked to calculate how to make a horse run faster?

“First of all, assume a spherical horse.”

Outline of Talk:

Jets are ubiquitous:

- star-forming regions – see, e.g., N. Panagia 2004
- galactic binaries & microquasars – see S. Chaty's talk
- active galaxies and quasars – see Josep Paredes' talk
- clusters of galaxies – see, e.g., Beall et al. 2005 in press.

Association of jets with accretion disks – see, e.g., Beall, 2003, Marscher, 2005 in press.

Association of jets in supernovae with GRBs – see, e.g., Gennadi Bisnovatyi-Kogan's talklater this morning, and Arnon Dar's talk this afternoon.

Outline of Talk (continued):

Some general remarks on jets and jet formation in accretion disks (see, e.g., Beall, 2003, Marscher, 2005 in press).

Take a close look at two systems:

- one galactic binary (Sco X-1) using VLBI data (from Fomalont, Geldzahler, and Bradshaw, 2001). Sco X-1 behaves very much like a microquasar.

- compare with 3C120 (using Alan Marscher and Jose-Luis Gomez, et al. data)

Outline of Talk (continued):

Discuss the role of plasma processes in the jet interactions with the interstellar and intracluster medium (see, e.g., Beall et al. 2005 in press.

Comment on neutrino flux from jets.

n.b.: Assuming a spherical horse is no longer sufficient.

Jets are a laboratories
- or at least experimental fields:

Nice confirmation of special relativity, both in terms of Doppler boosting and superluminal expansion.

When coupled with black hole/neutron star origins, jets have implications for testing general relativity.

Can use observations to test the connection of galactic jets to jets in AGN and quasars (over an enormous dynamic range).

Open Questions:

What are the jets made of?

Do the jets evolve as they propagate?

What are the specific mechanisms that
    accelerate the jets

How do the jets interact with the ambient
    medium and transfer energy to it?

Energy available from accretion onto a compact object

Accretion onto a compact object represents the most plausible source for the power in many astrophysical settings, including AGN, because of the efficiency of the accretion process relative to the rest mass energy of the object. This is so, somewhat surprisingly, even though the nuclear force is the strongest force and gravity is the weakest. The kinetic luminosity released by accretion is

$$dE/dt \sim (GM(dm/dt))/r \tag{1}$$

where M is the mass of the compact object, G is the gravitational constant, dm/dt is the accretion rate, and r is the radius at which the energy is released.

The escape velocity, v, is related to the mass of the attracting body by the

$$(1/2)mv^2 \sim GMm/r, \tag{2}$$

and for a compact object, $v \sim c$, i.e., the speed of light. Therefore,

$$dE/dt \sim \eta(1/2)(dm/dt)c^2 \tag{3}$$

where η is an efficiency factor usually taken to be $\sim 10\%$, and c is the speed of light. The efficiency for nuclear reactions is $\sim 1\%$.

Of course, accretion-powered sources include astrophysical jets.

see, e.g., Beall, J.H., 2001, Proceedings of the Vulcano Workshop

Jets in star-forming regions

Jets in Star-forming Regions in Molecular Clouds: There is evidence for accretion disks in the existence of bipolar outflows and in the agreement between calculated and observed spectra in giant molecular clouds. (see, ``The Observational Appearance of Protostellar Accretion Disks," in Beall 1987, Ap.J. 316, 227). Data on rho Ophiuchus taken from K. Tachihara's Ph.D. Thesis,

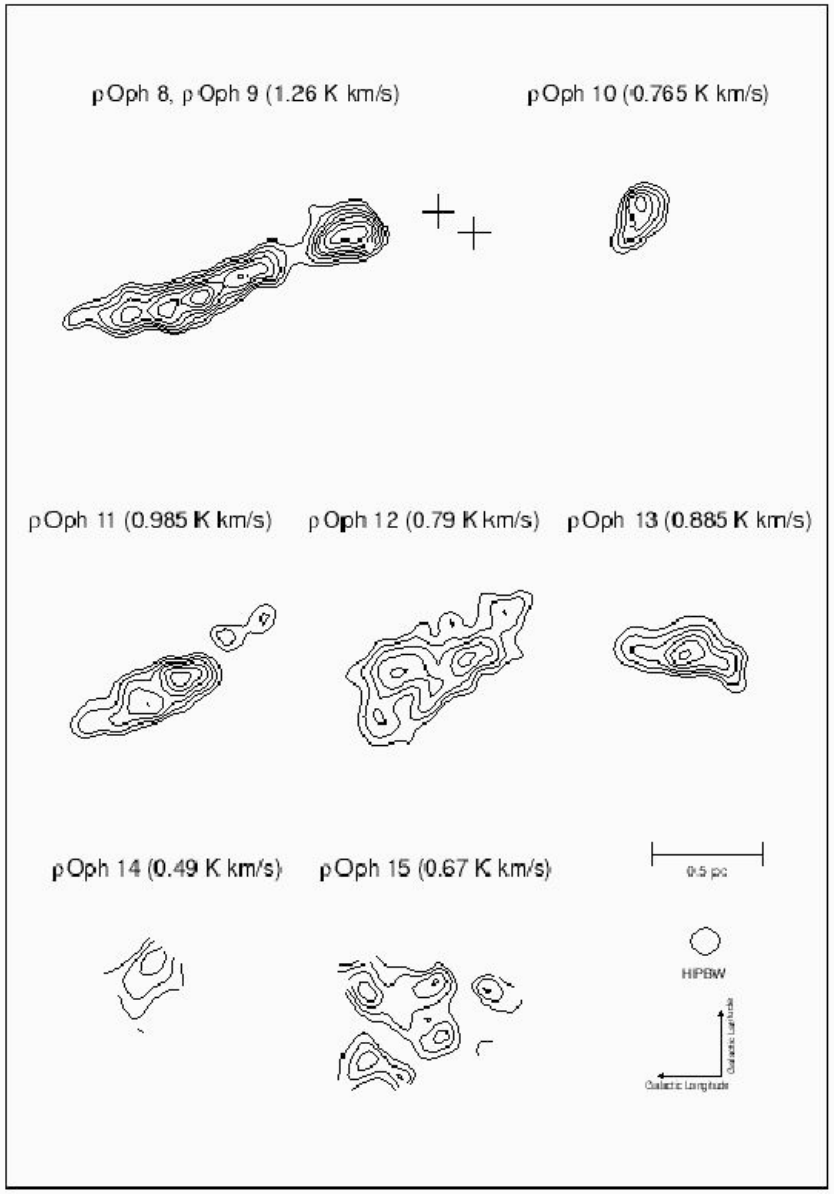

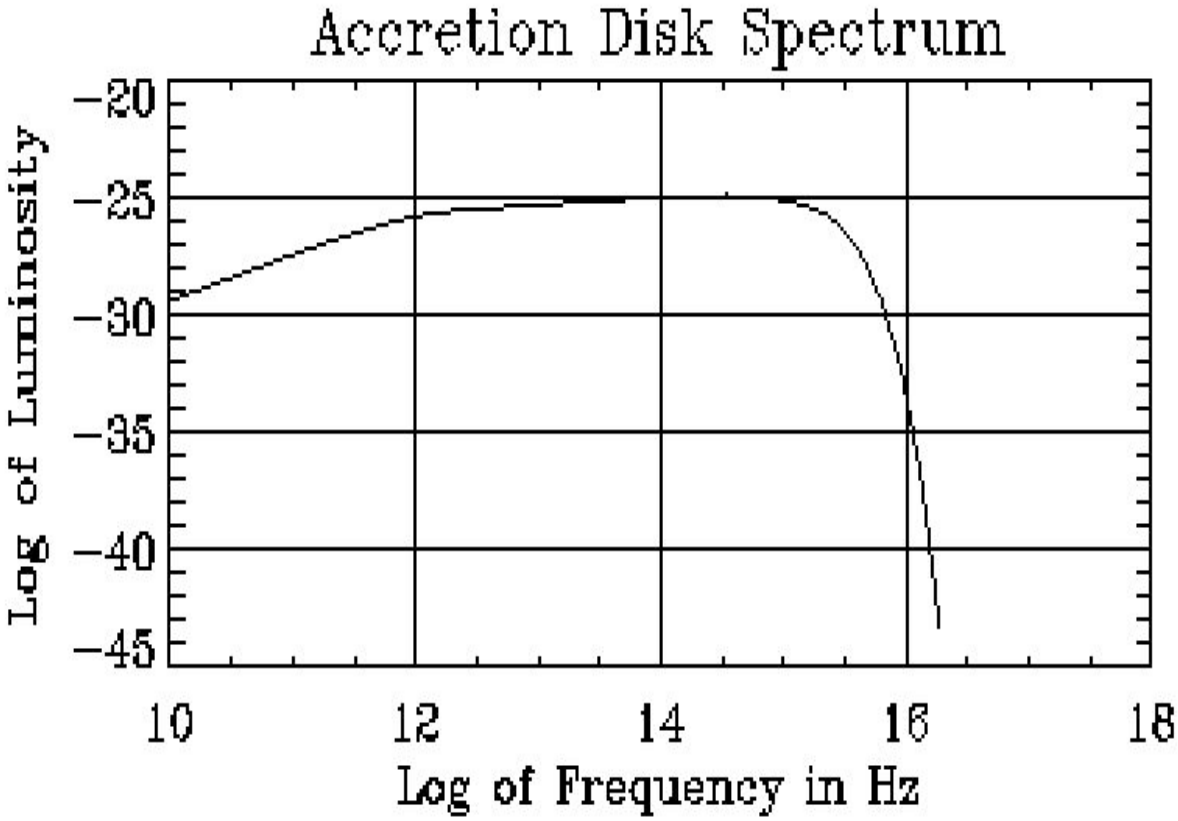

Calculation of accretion disk thermal spectrum

(after Beall, J.H., 1987 ApJ, 316, 227)

Thermal disk spectrum combined with Comptonized, soft x-ray photons upscattered to hard x-rays and gamma-rays (adapted from Hannikainen (2005)

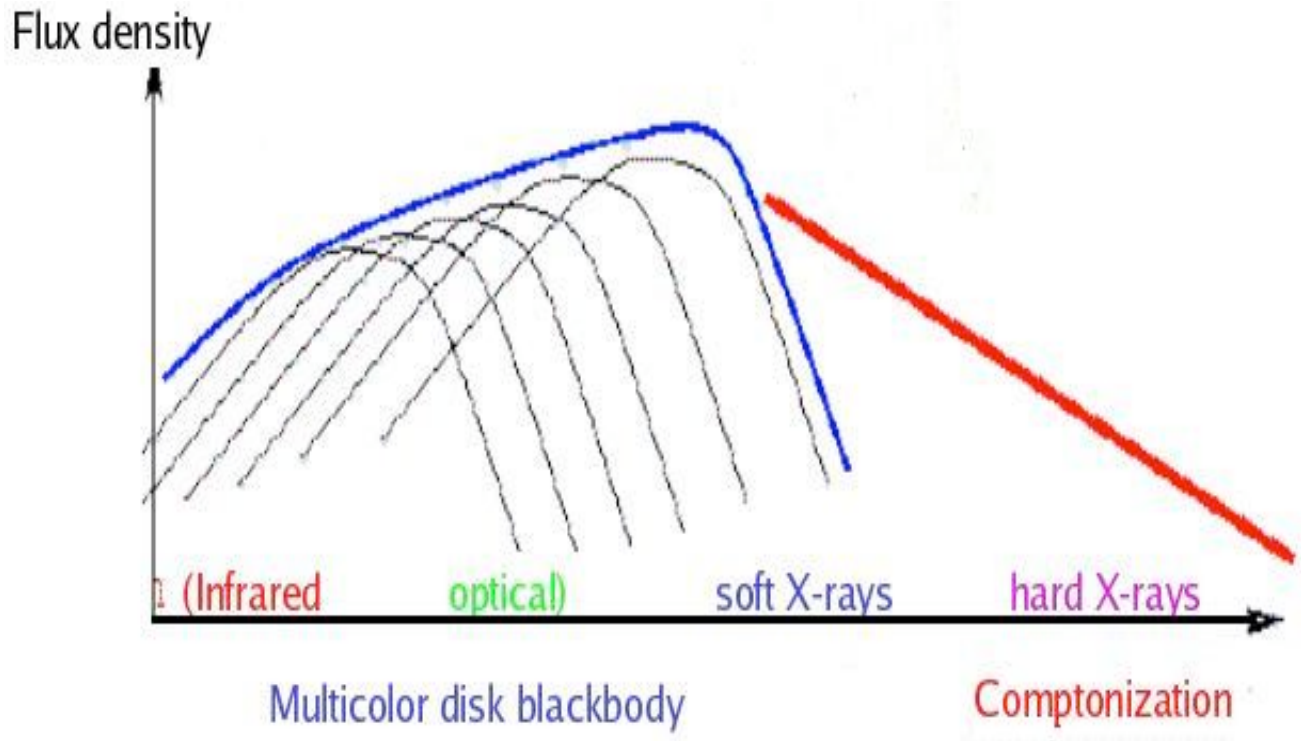

Comparison of Microquasars and Quasars (adapted from Mirabel)

AGN/Quasar Microquasar

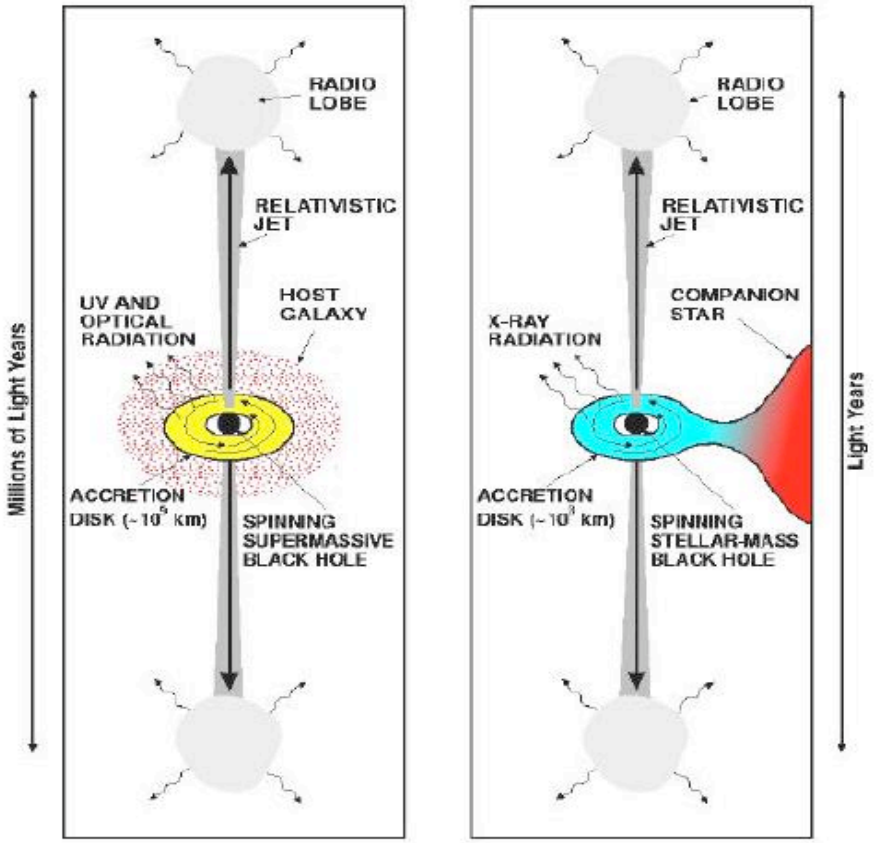

- Quasi-stellar relativistic object may be a Neutron Star or a black hole (BH)
- In BHs the scales of length and time are proportional to the mass of the BH
- The maximum color temperature of the accretion disk is $T_{col} \alpha (M/10M_{\odot})^{-1/4}$

ARE THERE BLACK HOLES WITH MASSES IN THE RANGE OF 10^2- $10^5 M_{\odot}$?

The central engine of an AGN:

Note the accretion torus with the Broad Line Region (BLR) clouds orbiting around the black hole and the accretion disk, the Narrow Line Region (NLR), and the jet of material propagating through central region and outward.

Below: Cen A core, R. Kraft et al. 1999, 2000

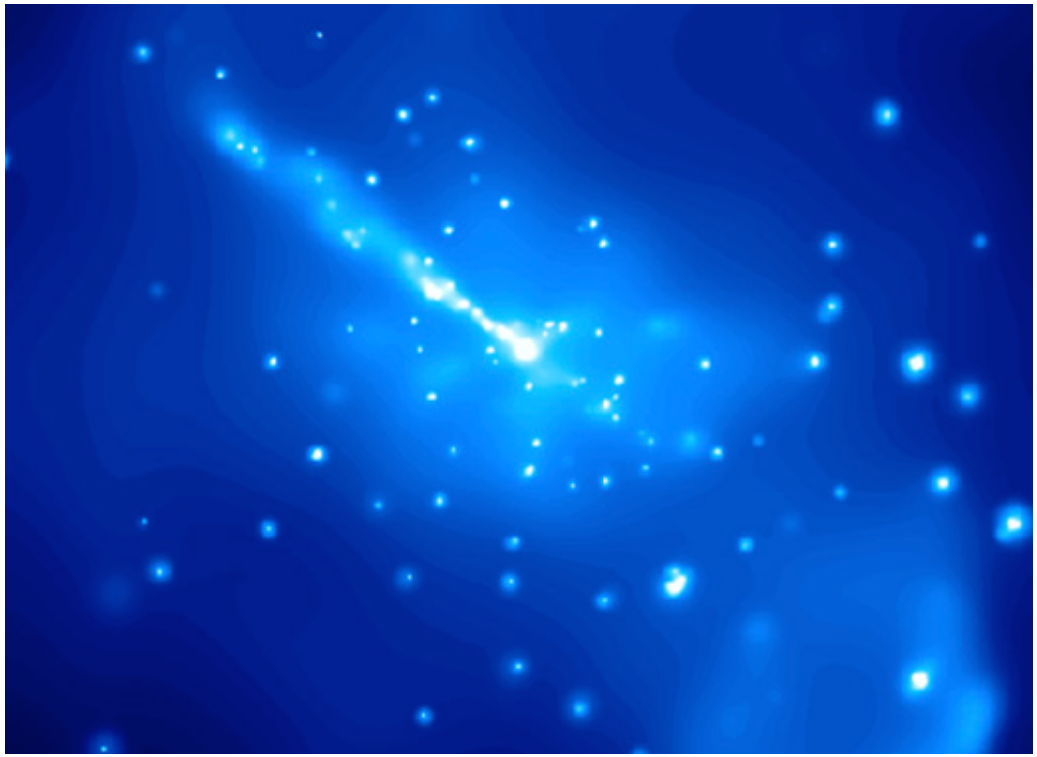

AGN schematic

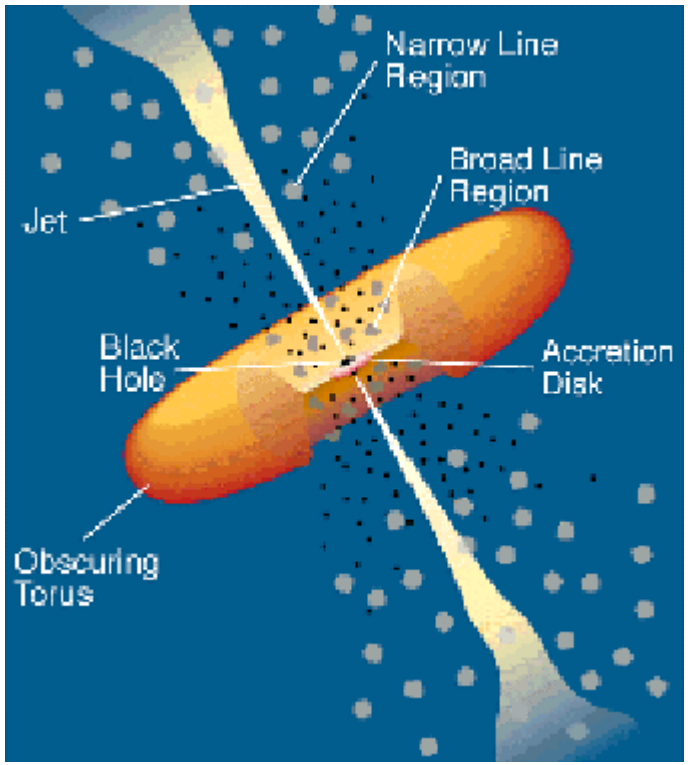

Multi-Frequency Image of M87 Jet Structure

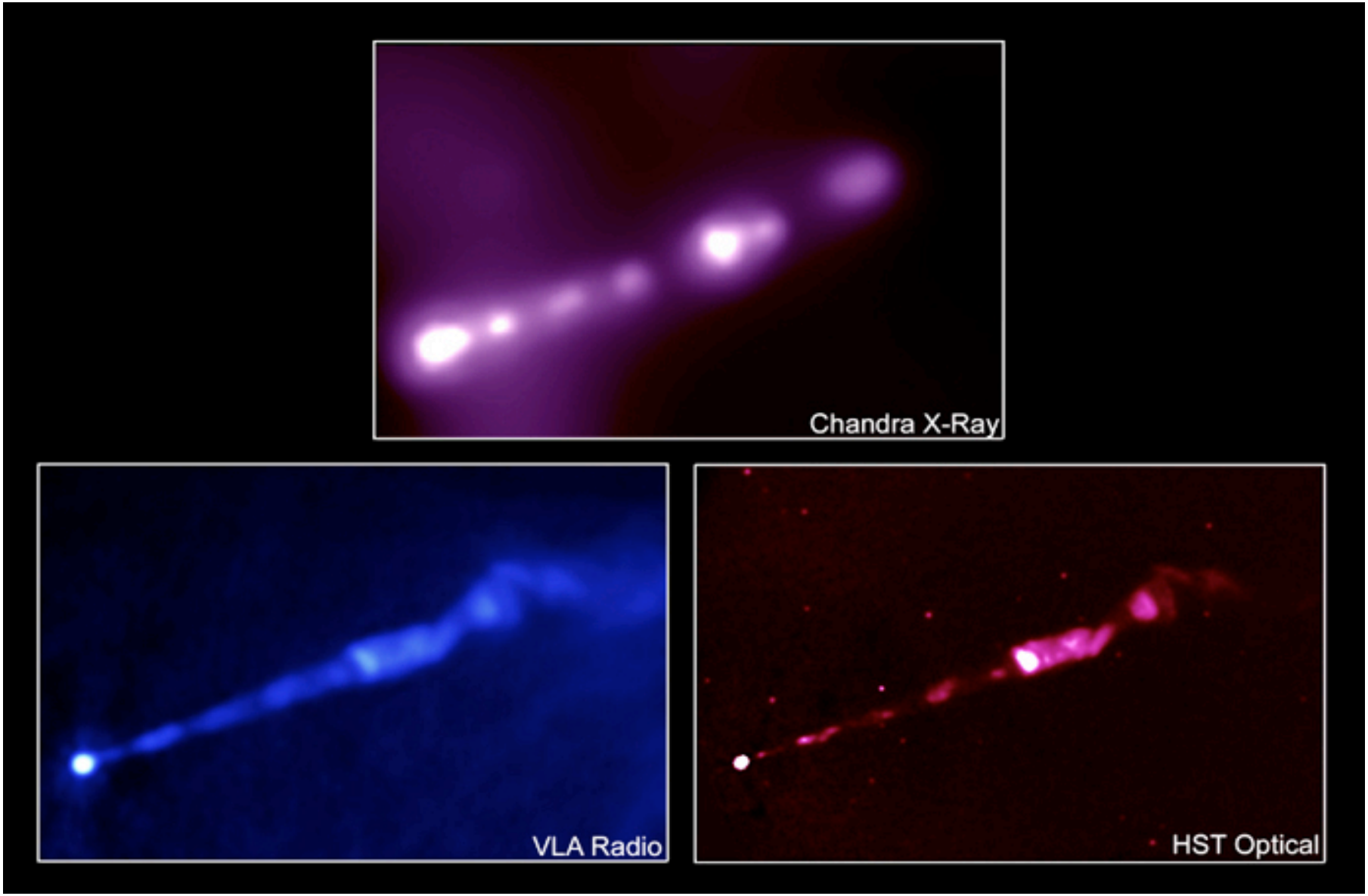

M87 at mas resolution (white bar is .01 pc)

Junor, Biretti, and Livio, Nature 1999, 401, 892

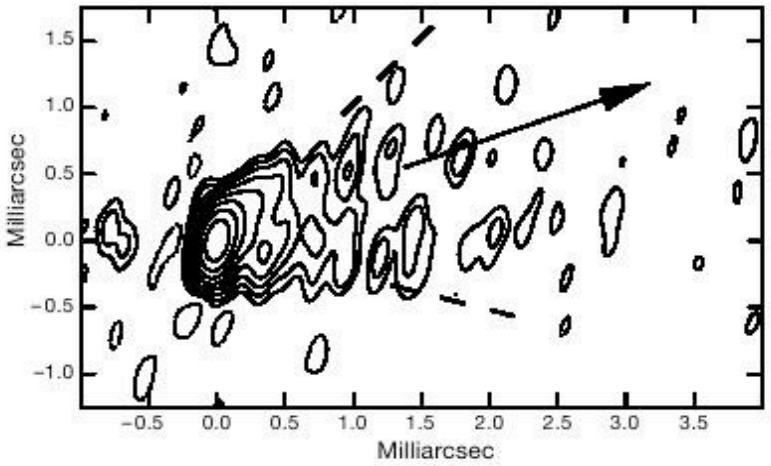

Figure 1 Image of the nucleus of M87 at 43.237 GHz on 3 March 1999. The synthesized beam is 0.33 mas × 0.12 mas (1 mas is 0.071 pc at the distance of M87) with the major axis in position angle −12.3°. The peak brightness in the image is 228 mJy per beam and the r.m.s. noise in the image well away from the bright structure is 0.38 mJy per beam. Contours are plotted at −1, 1, 2, 4, 8, 16, 32, 64 and 128 mJy per beam. The solid arrow indicates the direction of the 20″ jet, while the dashed lines indicate the position angles of the limb-brightened structure within 1 mas of the core. The antenna array consisted of the 10 telescopes of the Very Long Baseline Array (VLBA), 13 telescopes of the Very Large Array (VLA) phased together, and telescopes located at Effelsberg (Germany), Medicina (Italy), Metasahovi (Finland), Onsala (Sweden) and Yebes (Spain). Left circular polarization data were recorded at each telescope using 8 channels of 8 MHz bandwidth and 2 bit sampling. The data were correlated at the VLBA correlator, and later transferred to the AIPS package for calibration of the complex visibilities and imaging in a standard manner[25]. The complex visibility data have been weighted by the inverse fourth power of the signal-to-noise ratio of the complex visibility to improve the contribution of the higher spatial frequencies to the image.

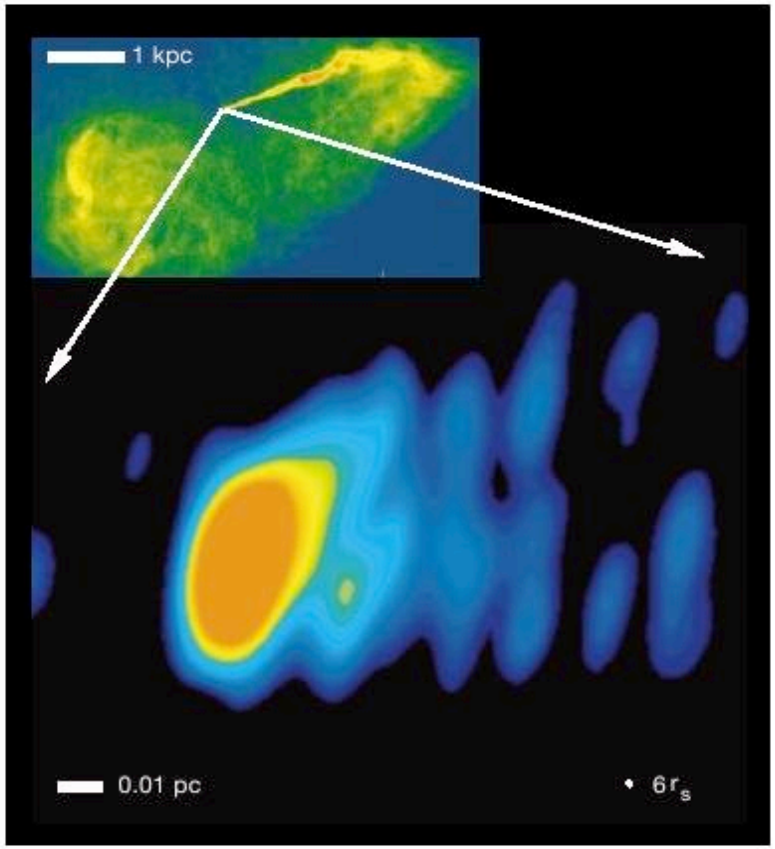

Figure 2 Pseudo-colour rendition of the nucleus of M87 at 43 GHz on 3 March 1999. See Fig. 1 for details. The filled white circle at lower right indicates $6r_S$, which is the diameter of the last stable orbit around a non-rotating black hole. The inset (top left) is a 15-GHz VLA image illustrating the large-scale jet.

Spatial and temporal evolution of 3C120 in VLBI radio and x-ray

- Radio brightness of the jet shown as contours.
- Color-coded contours represent the intensity of polarized radio waves.
- Strong polarization indicates well-ordered magnetic fields (the sticks are in the direction of the magnetic field).
- Bright "knots" appear and move down the jet, with their polarization changing.
- Red area with the black center represents the accretion disk .
- Light curve shows X-ray brightness varying with time. When the X-ray brightness decreases, the dark part of the accretion disk is illustrated as becoming larger.. About 4 weeks later, the “starting point” of the jet gets bright and a new superluminal knot moves down the jet.

Red ellipse represents inner accretion disk. Contours = 43 GHz intensity. Inset: X-ray light curve (data courtesy of Alan Marscher and Jose-Luiz Gomez) 1 mas = 0.70 pc @ D = 120 Mpc. (see Gomez et al. 2000 Science, 289, 2317)

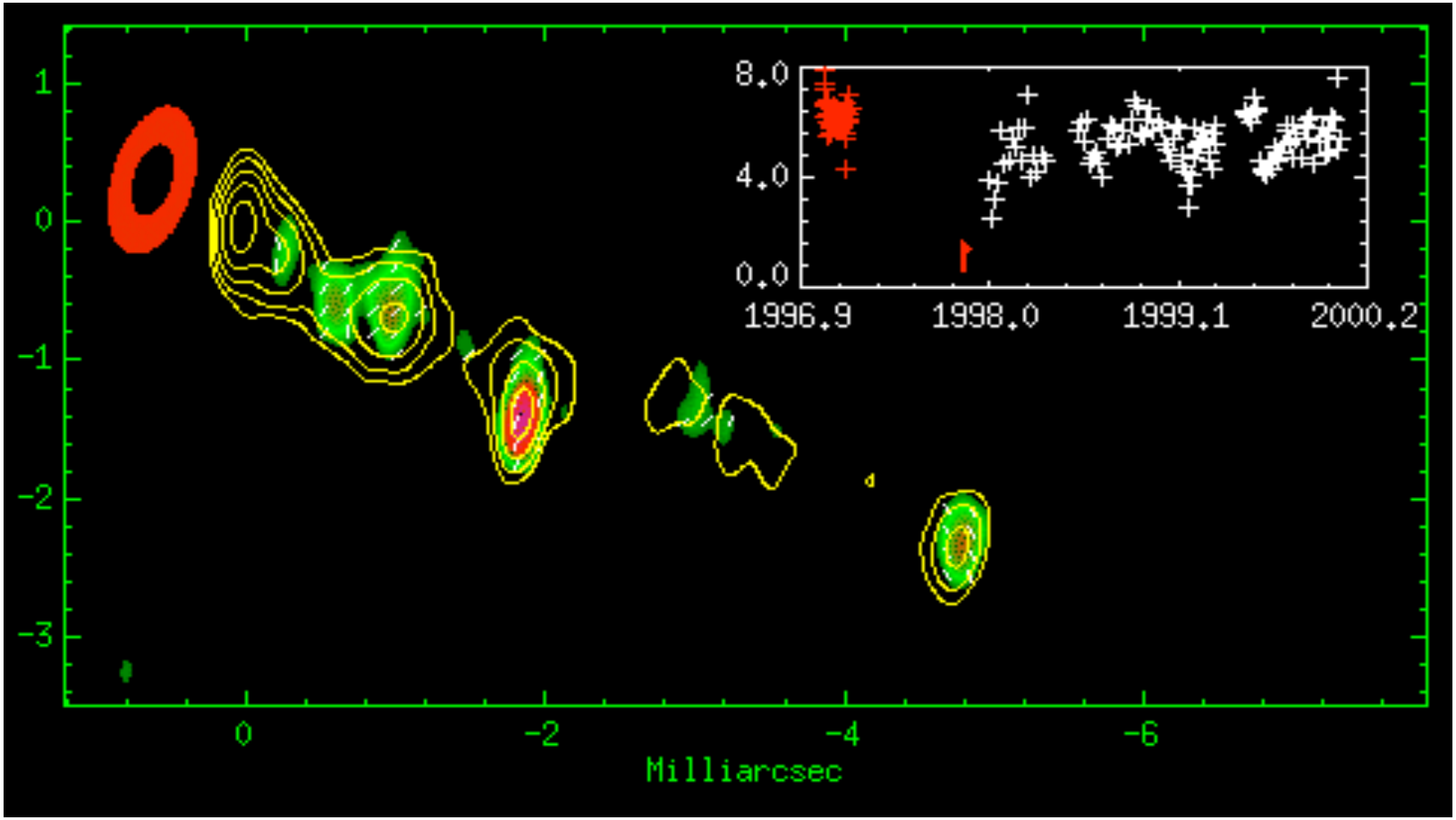

Sco X-1 frames from "Movie" (see Fomalhaut, Geldzahler, and Bradshaw, 2001 Ap.J., 558, 283). For large "blobs", v = .45c. On this scale, 1 mas = 2.8 AU = 4.19×10^{13} cm with Sco X-1 at a distance, D = 2.8 Kpc (9000 light years).

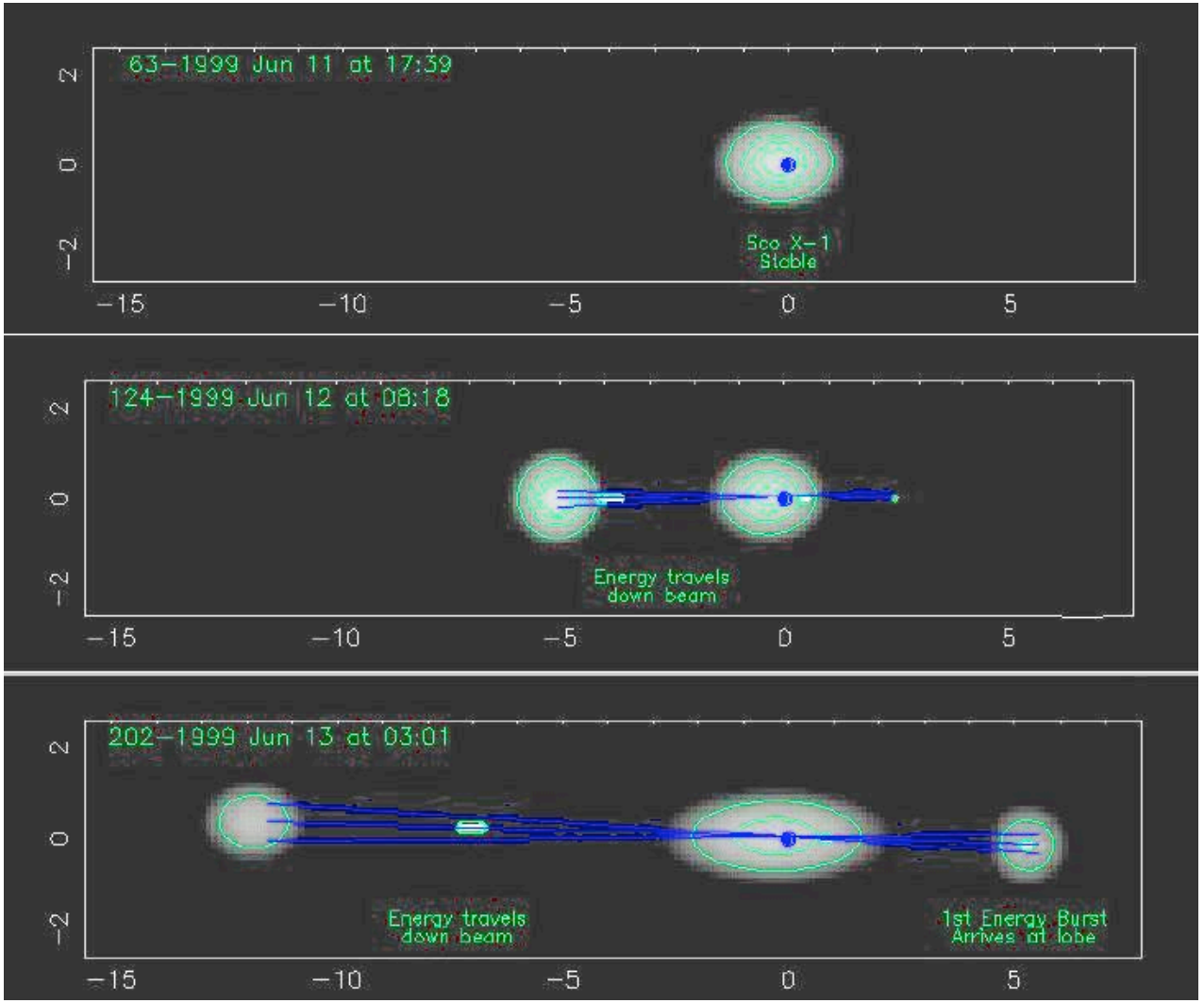

Sco X-1 “Movie” (see Fomalhaut, Geldzahler, and Bradshaw, 2001 Ap.J., 558, 283, and Beall, 2003 for discussions). Note that Sco X-1 is a neutron star (1 mas = 2.8 AU = 4.19×10^{13} cm).

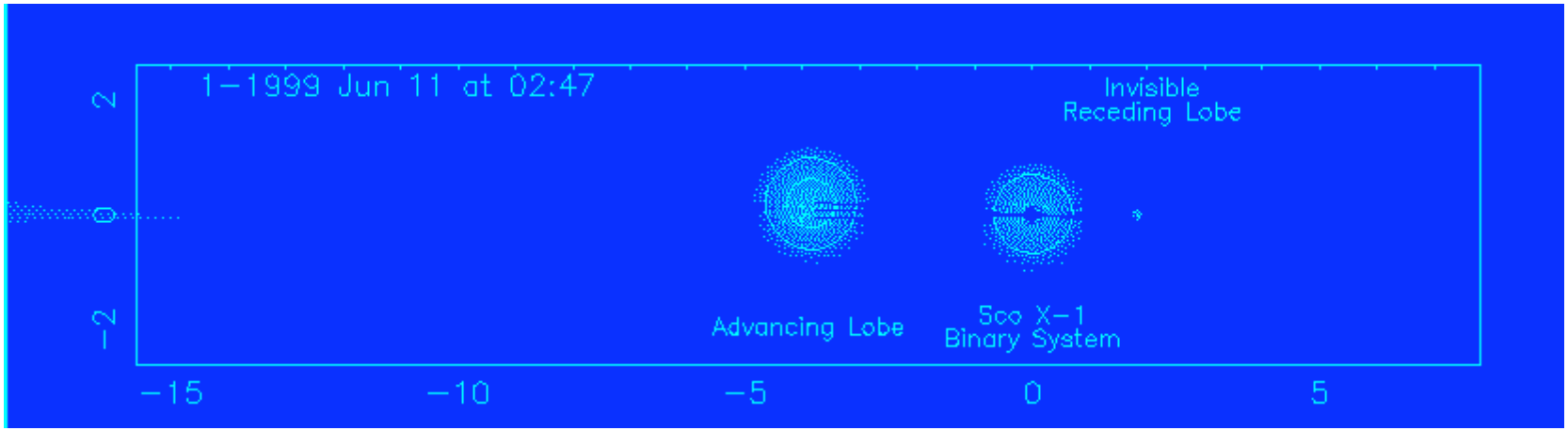

These data show a time-lapsed interval from 0400 UT, 11 June 1999 through 0900 UT, 13 June 1999, that is, roughly two days.

Enhancement of VLBI using Satellite-based Arm

Ground-Space-Based VLBI gives a factor of **10 better resolution**. The VSOP mission is a Japanese-led project to image radio sources with sub-milliarcsec resolution by correlating the signal from the orbiting 8-m telescope, HALCA, with a global array of telescopes. Twenty-five percent of the scientific time of this mission is devoted to a survey of 402 bright, small-diameter extra-galactic radio sources at 5 Ghz. (Hiribayashi et al. 2000 PASJ, 52..997H)

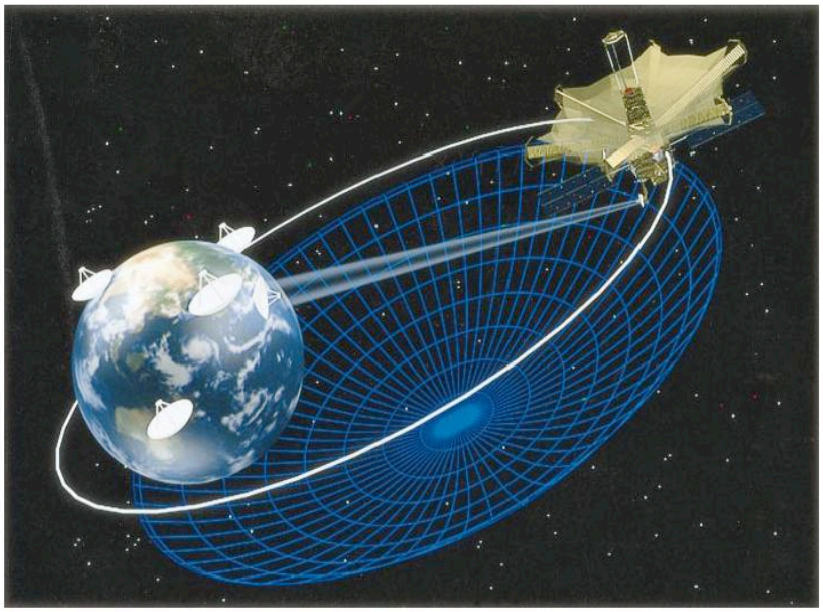

Fig. 1. An artist's impression of HALCA co-observing with ground-based radio telescopes to create a radio telescope that is much larger than that achievable on Earth only.

Jets in Clusters of Galaxies

A number of mechanisms have been proposed for heating of the intracluster gas in clusters of galaxies.

Shock heating (Inoue and Sasaki, 2002; Zanni, et al., 2005)

Heating via plasma processes (Beall et al., 2005)

Chandra Image of MS0735.6+7421 Showing Cluster Holes

Jets can travel outward from the central engines of AGNs to distances > 100's of kiloparsecs.

In Cen A, the luminosity of the central engine, maintained over the propagation time scales of the jet required to form the giant radio lobes, can supply the energy of 10^{60} ergs that is present in those radio lobes (Beall and Rose, 1981).

It is possible that the cluster holes in this CHANDRA image of MS0735 +7421, have been formed by jets,

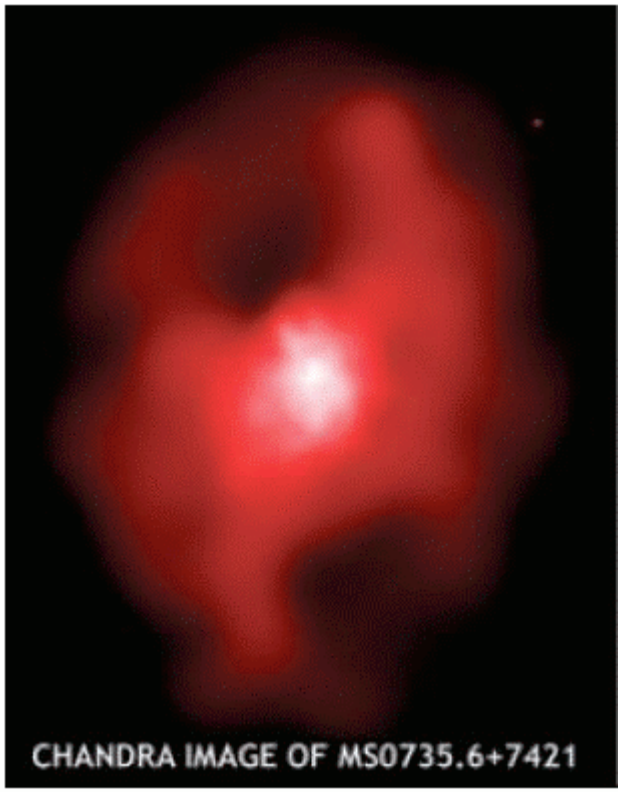

The environment that the jets propagate through is enormously complex. The range of densities involved in the interaction varies over many orders of magnitude, and the jet itself clearly evolves by a number of mechanisms:

- Energy loss by various loss mechanisms*
- Entrainment of the ambient medium contributes to the makeup of the jets,
- The changes in the jets' constitution through losses and acceleration of particles.

(see, e.g., Scott Holman, Ionson, and Papadopoulos, 1980 Ap.J. 239, 769, Rose, Guillory, Beall, and Kainer, 1984 Ap.J., 280, 550; and Beall 1980 in *Physical Processes in Hot Cosmic Plasmas*, Kluwer Pub.).

The environment that the jets propagate through is enormously complex. The range of densities and scale lengths involved in the interaction varies over many orders of magnitude.

This leads to an additional question: Are there **self-similar structures** at these different scales in individual jets and in galactic vs. extragalactic jets, and does that suggest an avenue for investigation?

(see, e.g., Scott Holman, Ionson, and Papadopoulos, 1980 Ap.J. 239, 769, Rose, Guillory, Beall, and Kainer, 1984 Ap.J., 280, 550; and Beall 1980 in *Physical Processes in Hot Cosmic Plasmas*, Kluwer Pub.).

Comments on Modelling: Much of the detailed physics of the jet-ambient-medium interaction is left out of even magneto-hydrodynamic models. These interactions can be properly modelled by Particle-in-Cell (PIC) codes. However, PIC codes are enormously computer-intensive, since they in effect model the detailed electromagnetic interactions of each particle with those within its "neighbourhood," i.e., its Debye length.

Multi-scale codes can overcome this by modelling the microscopic interactions as a population-predation interaction (which runs much faster). We can then calculate the **energy deposition rate, momentum transfer rate, and consequent heating**, and provide these as inputs into the magneto-hydrodynamic code to solve the multi-scale evolution of these jets.

What mechanisms work to deposit energy in the ambient medium as the jet propagates through it, and how does the jet maintain its coherence as it propagates such remarkable distances?

We posit a relativistic jet of either e^- - e^+, p – e^-, or more generally, a charge-neutral, hadron – e^- jet. The jet has a significantly lower density than the ambient medium.

Initially, and for a significant fraction of its propagation length, the principal energy loss mechanisms for such a jet interacting with the ambient medium is via plasma processes*.

*see, e.g., Scott Holman, Ionson, and Papadopoulos, 1980 Ap.J. 239, 769, Rose, Guillory, Beall, and Kainer, 1984 Ap.J., 280, 550; and Beall 1980 in *Physical Processes in Hot Cosmic Plasmas*, Kluwer Pub.).

Jet-Ambient-Medium Interaction

The primary energy loss mechanism for the electron-positron jet is via plasma processes:

- The two stream instability
- The oscillating two stream instability
- Ion-acoustic waves

These instabilities set up waves in the plasma which produce regions of high electric field strength and relatively low density, called “cavitons” (after “solitons” or solitary waves), which propagate like wave packets in quantum mechanics.

These mix, collapse, and reform, depositing energy into the ambient medium, transferring momentum to it, and entraining (i.e., dragging along and mixing) the ambient medium within the jet.

Jet-Ambient-Medium Interaction (continued)

Particle-In-Cell (PIC) code simulation of an electron-positron jet propagating through an ambient medium of an electron plasma. A small magnetic field is applied along the jet's longitudinal axis to suppress a filamentation instability.

This shows that a relativistic, low-density jet can interpenetrate an ambient gas or plasma.

Note the initial build-up of the plasma waves in the jet and ambient plasma to the right of the slide.

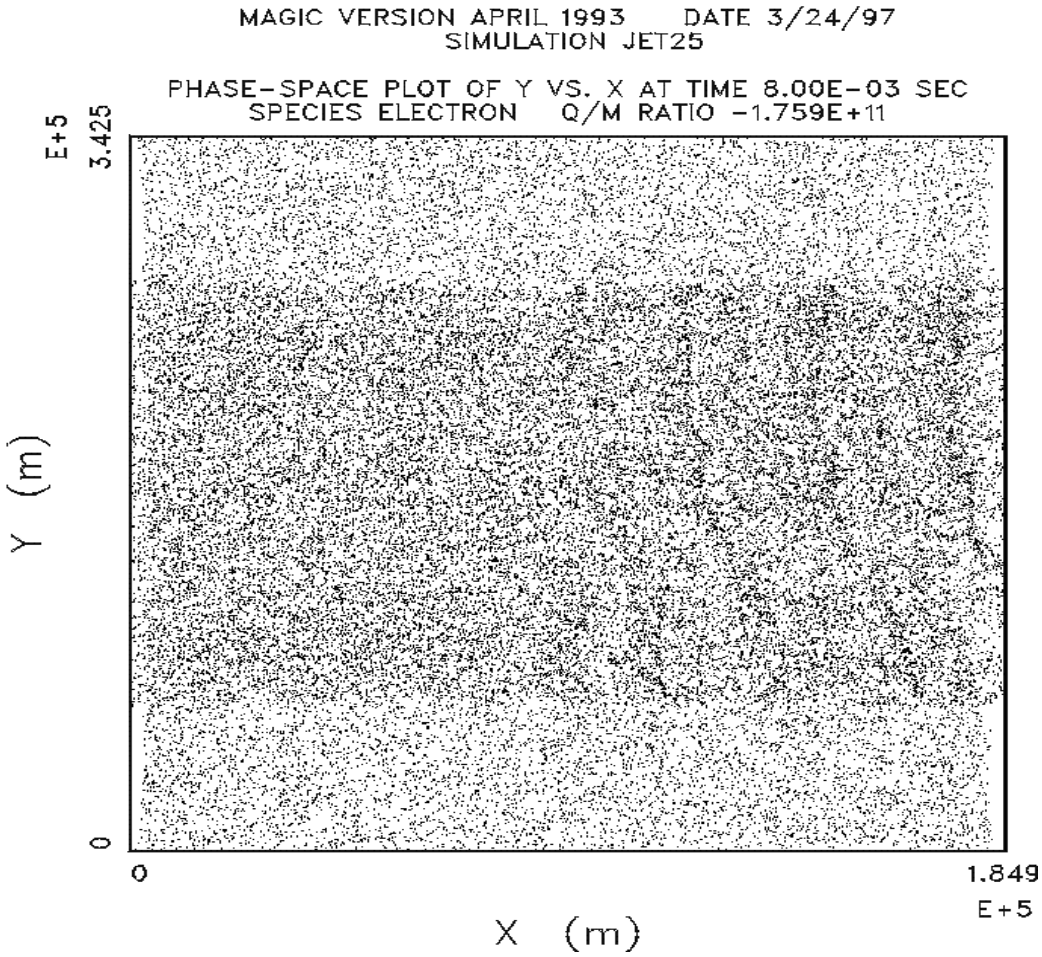

Jet-Ambient-Medium Interaction (continued)

In order to determine the energy deposition, momentum transfer, and heating, we model the plasma interaction as a system of coupled differential equations.

The solution to these equations gives a normalized wave energy. This wave energy density is then used to determine:

- the energy deposition rate of the jet into the ambient medium,
- the propagation length,
- the heating of the plasma, and
- the momentum transfer rate.

The plasma wave interactions are similar to a predator-prey system

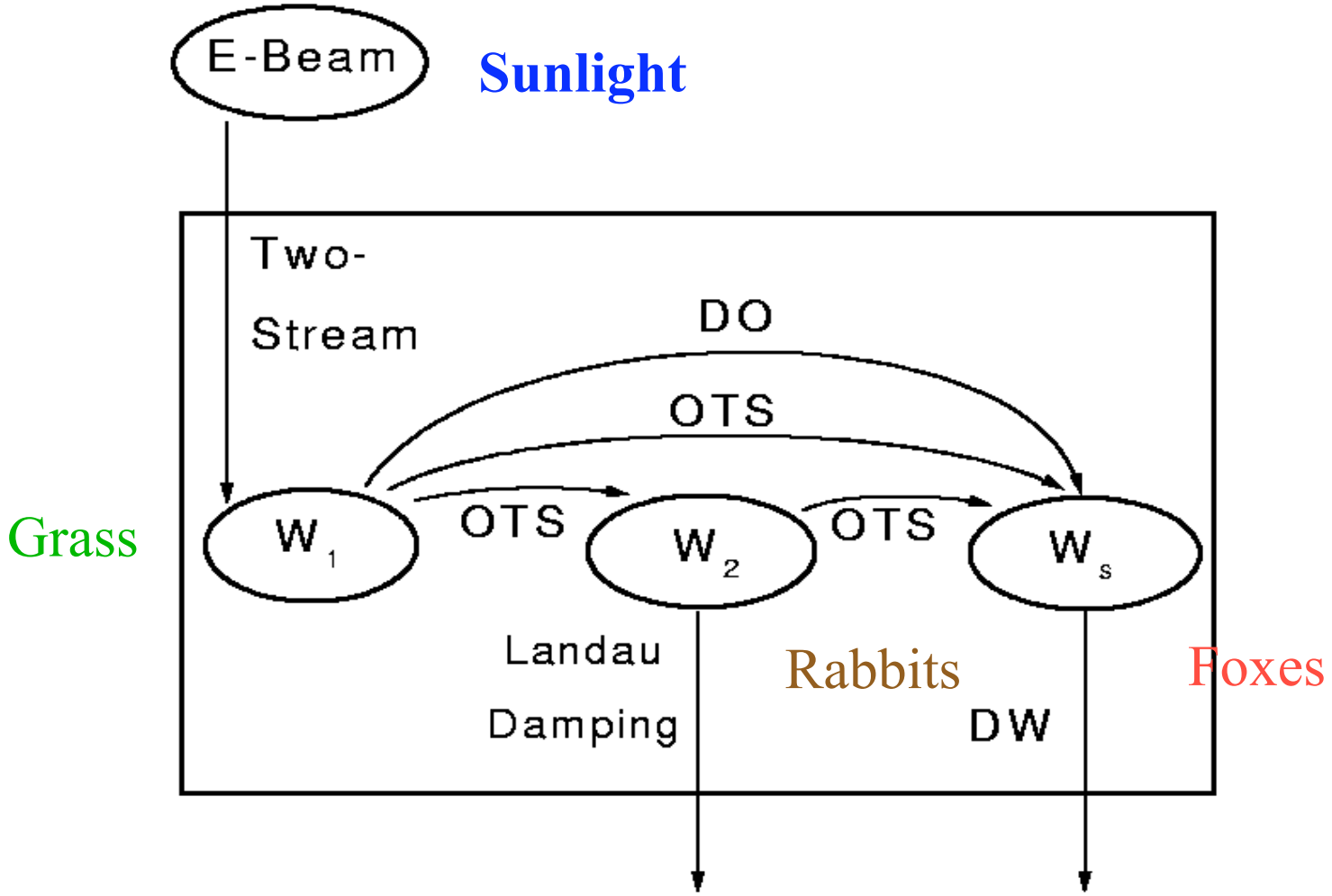

Wave Population Rate Equations: a system of coupled, differential equations that model the plasma interactions with the ISM/ICM

$$\frac{\partial W_1}{\partial t} = \left[2\Gamma_1 W_1 H\left(\frac{\epsilon_w}{n_p T_e} - W_1\right)\right] - \left[2\Gamma^{DO}(W_s)W_1 + 2\Gamma^{OTS}(W_1)W_2 H(W_1 - k_1^2\lambda_D^2)\right]$$

$$\frac{\partial W_2}{\partial t} = \left[2\Gamma^{DO}(W_s)W_1 + 2\Gamma^{OTS}(W_1)W_2 H(W_1 - k_1^2\lambda_D^2)\right]$$

$$- \left[2\Gamma_L W_2 + 2\Gamma^{OTS}(W_2)W_s H\left(W_2 - \frac{4}{\omega_p}\Gamma_L\right) + \frac{W_2}{\tau_2}\right],$$

$$\frac{\partial W_s}{\partial t} = \left[2\Gamma^{OTS}(W_1)W_s H(W_1 - k_1^2\lambda_D^2) + 2\Gamma^{OTS}(W_2)W_s H\left(W_2 - \frac{4}{\omega_p}\Gamma_L\right)\right]$$

Wave-population code shows quasi-equilibrium levels reached over short time periods

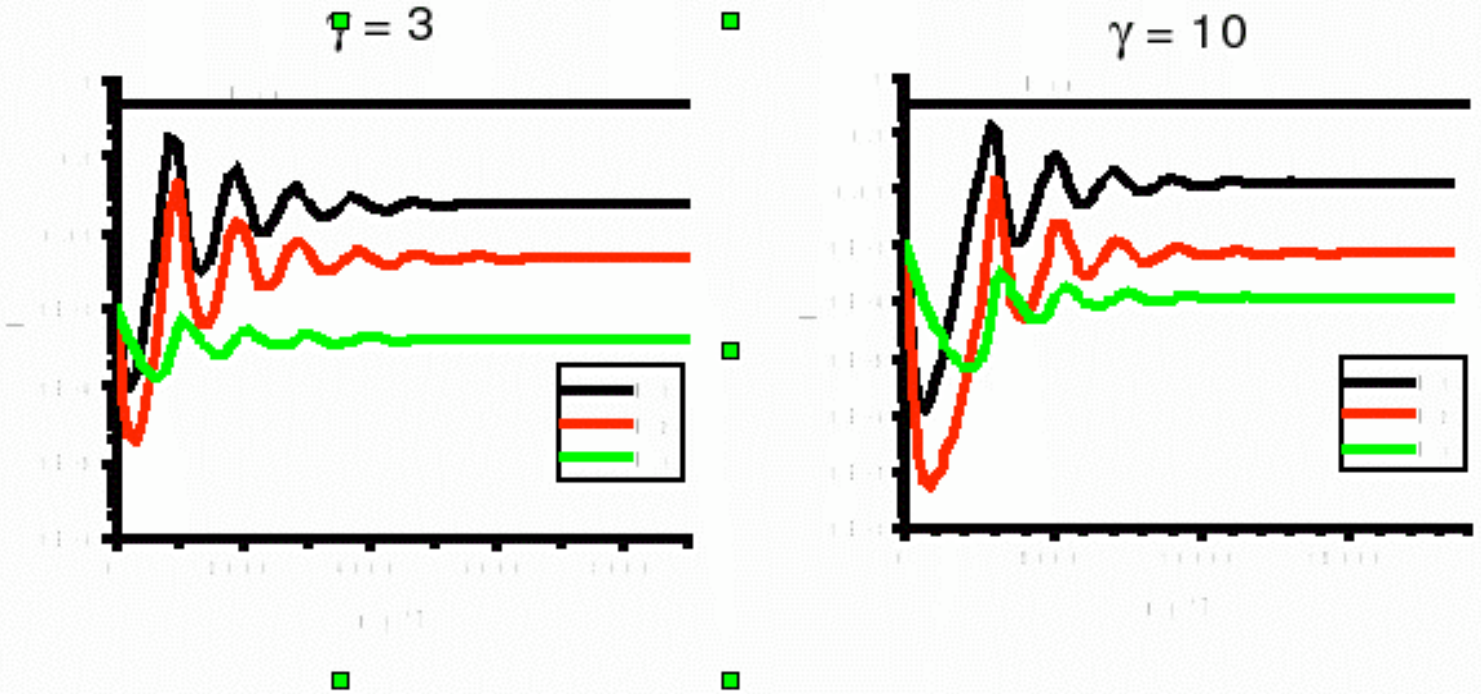

- n_p = 1 cm^{-3}, T_c=1 eV, R=10^{-4}, and f_h = 0.1

Collisionless (Plasma) Losses:

$dE_{plasma}/dx = -(1/n_b v_b)(d\alpha\epsilon_1/dt)$,

can be obtained by determining the change in γ of a factor of 2 with the integration:

$\int d\gamma = -\int [d(\alpha\epsilon_1)/dt]/(v_b n_b m^{'} c^2)$

as shown in Rose et al., 1978 and Beall 1990. Thus,

$L_p = ((1/2)\gamma c n_b m c^2)/(d\alpha\epsilon_1/dt)$

is the characteristic propagation length for collisionless losses for an electron or electron-positron jet. In many astrophysical cases, this is the dominant energy loss mechanism.

Energy Deposition Rate of Jet Energy Into Ambient Medium

The average energy deposition rate if given by the average normalized wave energy, W, as follows:

$$\langle d\alpha\varepsilon / dt \rangle = nkT \langle W \rangle \omega_p \text{ ergs cm}^{-3}\text{s}^{-1}$$

where n is number density of the ambient medium, <W> is the average normalized wave energy density obtained from the wave population code, and ω_p is the plasma frequency.

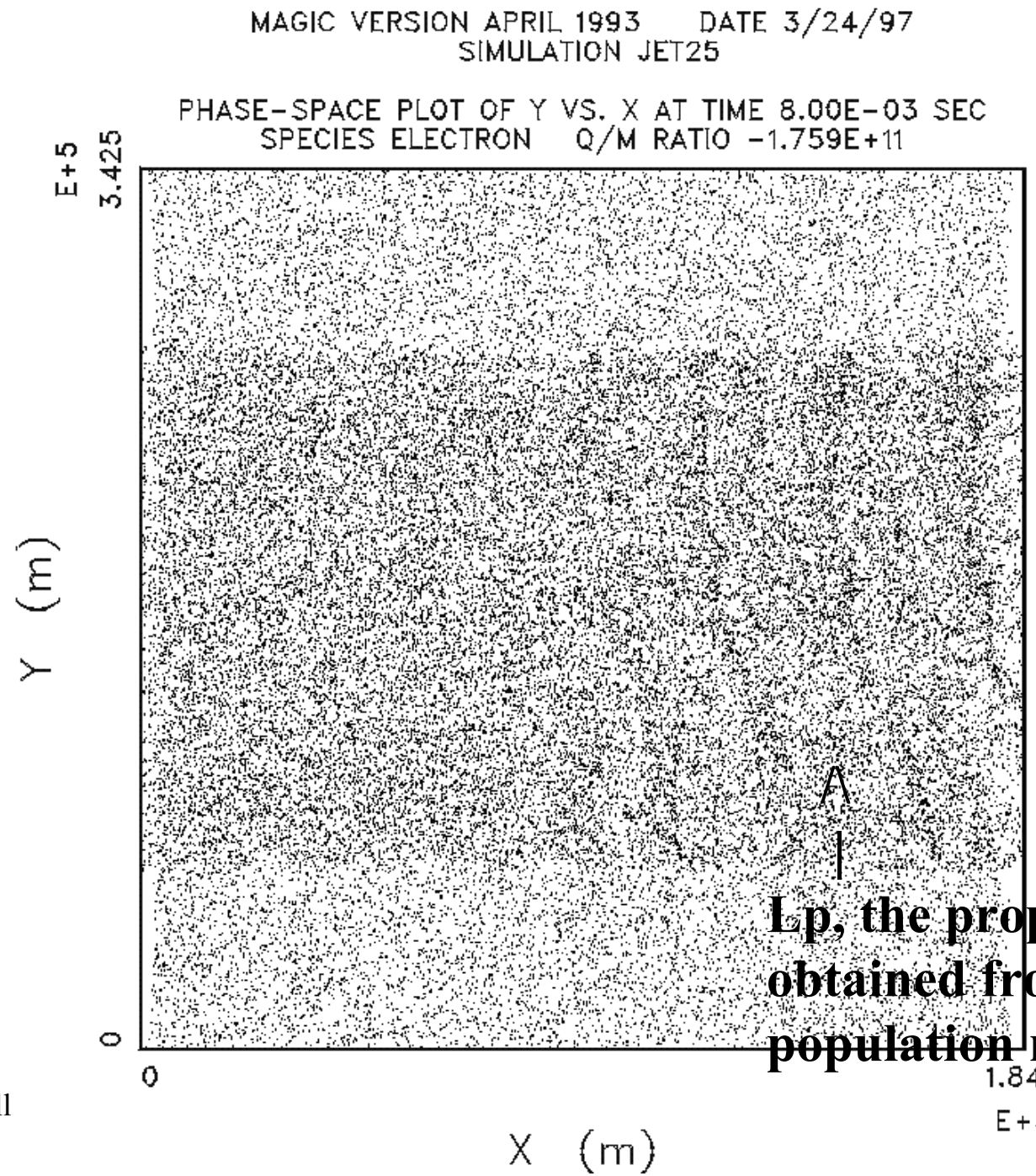

Lp, the propagation length obtained from the wave population model code

Note the jet energy loss, the heating, and entrainment of the ambient medium.

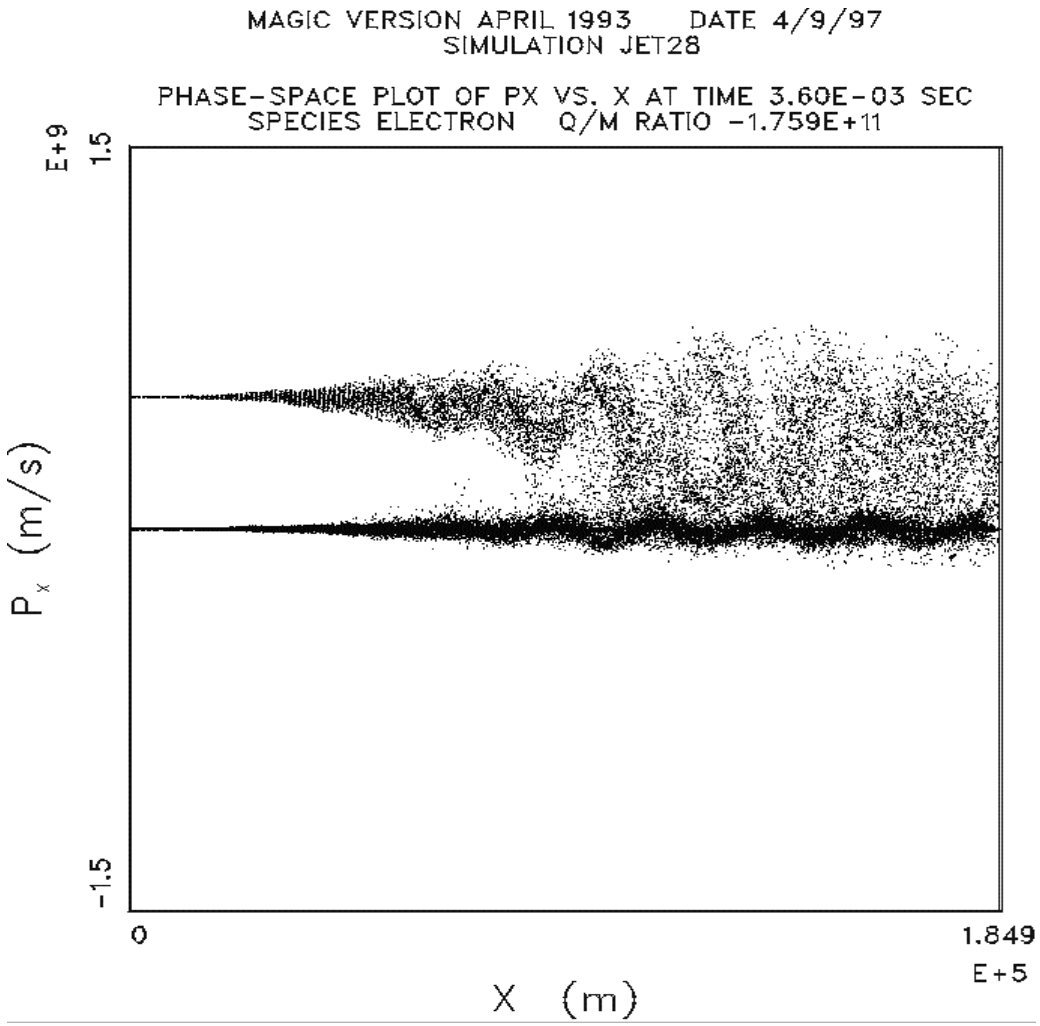

Detailed comparisons between wave-population model and particle-in-cell models in good agreement for specific parameter regimes:*

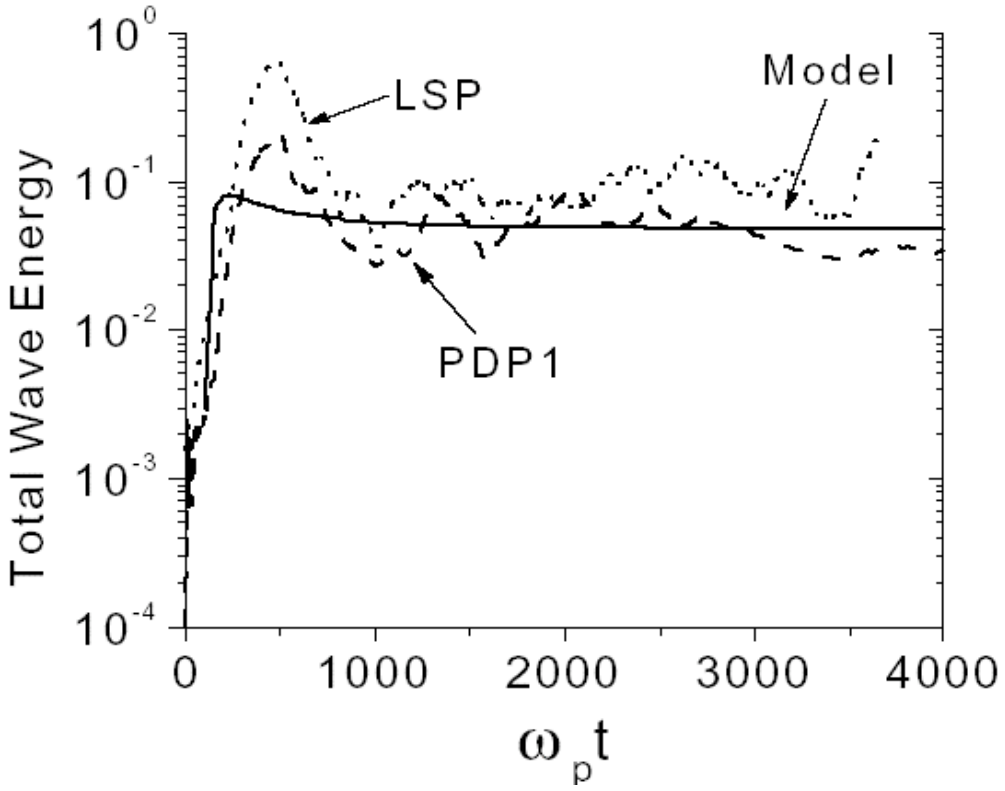

Non-relativistic 1D PIC simulations

Propagation length consistent with estimates of collisionless loss-rate estimates**

>200 particles per cell for good representation of distribution functions

*D. V. Rose, J. Guillory, J. H. Beall, *Phys. Plasmas* **9**, 1000 (2002).
*W. K. Rose, et al., *ApJ* **280**, 550 (1984).

Growth of a High Energy Tail on the Maxwell-Boltzmann Distribution of the Gas in the Ambient Medium

An analytical calculation of the "boost" in energy of the electrons in the ambient medium to produce a high energy tail with $E_{het} \sim 30 - 100$ kT is confirmed by PIC-code simulations.

n.b.: This can greatly enhance line radiation over that expected for a thermal equilibrium calculation.

Nonthermal electron tail evolution examined in PIC simulations

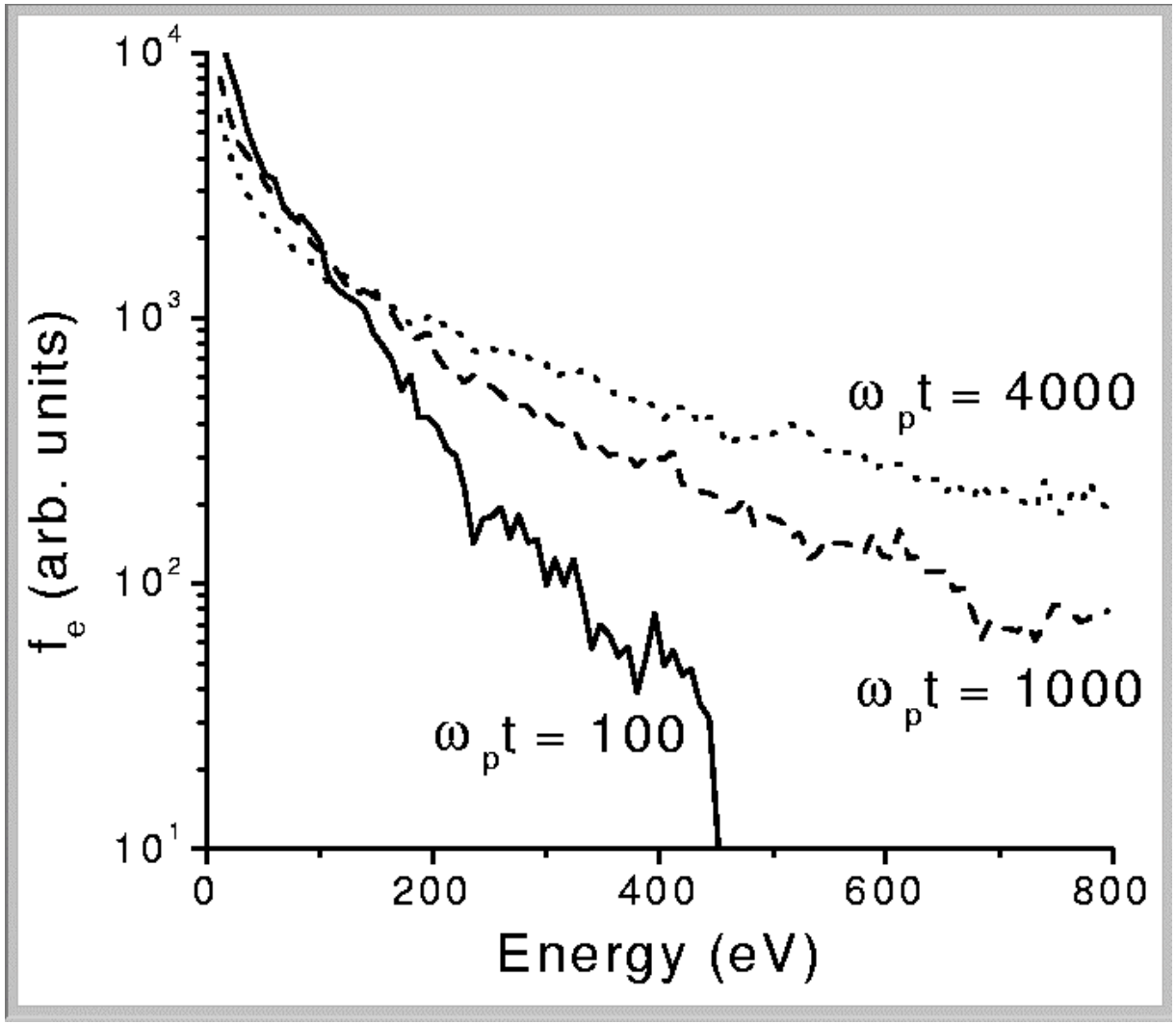

- Simulations track the evolution of the electron and ion distributions for an electron beam propagation in a dense (R=0.01) background plasma, where $R=n_b/n_p$

Line enhancements can result from the presence of a hot plasma electron tail:

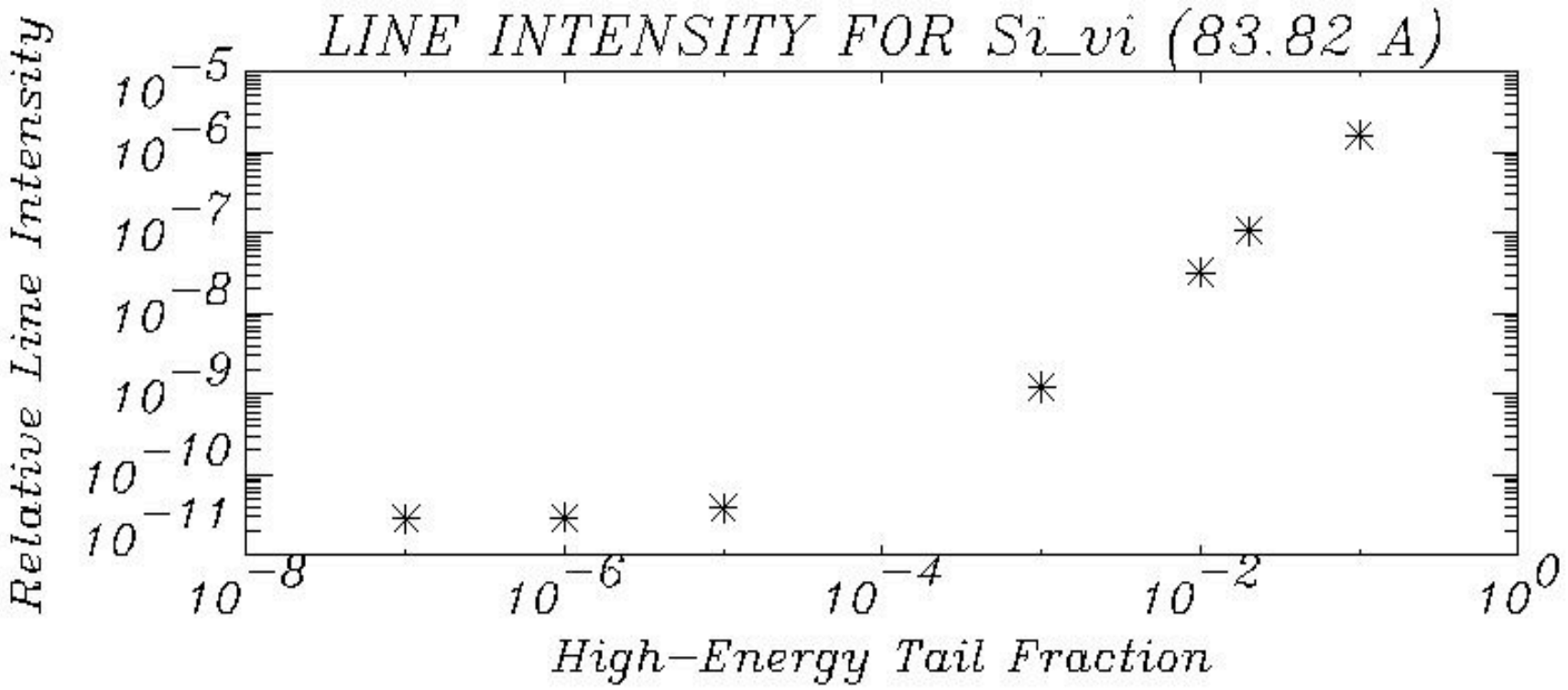

Illustrative calculation of line ratios for Si from the XSTAR code (T. R. Kallman & M. Baustista, Ap.J. 2001), modified to treat non-thermal temperature distributions (Guillory and Beall) induced by jet-ISM/ICM interaction

Jet Parameters from Kinetic Luminosity

We can further constrain the jet parameters by expressing the kinetic luminosity of the jet as

$$P_b = dE/dt = \gamma mc^2 n_b v_b \pi r_b^2, \tag{16}$$

where γ is the ratio of total energy to rest mass energy, mc^2 is the rest mass energy of the beam particles, v_b is the beam velocity, and r_b^2 is the beam radius.

Some points on propagation lengths for the jets.

The propagation length, Lp, depends nonlinearly on the jet Lorentz factor, γ, the jet particle number density, and the mass of the jet particles In addition, it depends in a complex way on the wave energy density,

$$<\alpha\varepsilon> = nkT <W> \text{ ergs cm}^{-3}$$

of the plasma waves. In general, the propagation length is greater for greater γ.

Though the plasma energy loss rate is determined by the collective (plasma) processes, the jet energy depends on the mass. A jet of hadrons will therefore propagate of order $2x10^3$ farther than an electron-positron jet and can produce a significant neutrino flux.

Some examples may be helpful.

Illustrations of Total Propagation Length for an Electron-Proton Jet:

For a cold beam with a beam radius, r_b=3x10^19 cm, the temperature of the ambient medium, T_c=1x10^4K, a high-energy tail temperature, T_h=1x10^5K, a hot tail fraction, f_h=.10, n_{b}=.001, and n_p=.01, and: \gamma =100, the propagation scale length for an electron-proton jet, $L_pe-=9x10^20 cm (i.e., 300 pc), and an energy deposition rate, dE/dt=3.6x10^-15 ergs/cm^3s.

For \gamma = 1000, L_p ~ 3 kpc. Since L_p is the distance over which the jet looses energy by a factor of two. Therefor, **the total propagation length can be of order 10^3 kpc.**

For the same parameters but with n_p=.1, L_pe-=7x10^19cm (i.e., $\sim 20 pc), and dE/dt=2.4x10^{-15} ergs/cm^3s for \gamma = 100. For \gamma = 1000, L_p can be of order 200 pc, yielding a **total propagation length of order 100 kpc**.

Illustration of Gamma-ray Spectrum from Hadronic Interactions of Jets with the Ambient Medium. Preamble:

The gamma-ray spectra produced during propagation of relativistic electron-proton beam in the cloud with inclusion of collisionless losses. These results are shown for the power law spectrum of protons with the spectral index, alpha=2. (see (a), (b), and (c)) and normalization A = 10^4 (b), 10^5 (a,), and 10^6 (figures c,d). The proton beam propagates in the cloud with the density n_c = 10^{12} cm^{-3} (a,b,d), and n_c = 10^{13} cm^{-3} (c), and temperature T_c = 10^4 K, The specific curves correspond to different propagation distances
in the cloud L = 10^{12} cm (dashed curve), 3x10^{12} cm (full curve), 10^{13} cm (dot-dashed curve), and 3x10^{13} cm, accept (c) and (e) for which the propagation distances are an order of magnitude lower. The dotted curve shows the \gamma-ray spectrum in the case when collisionless losses are not included. (Beall and Bednarek, 1999)

Hadronic-Jet-Ambient-Medium γ–ray Spectrum

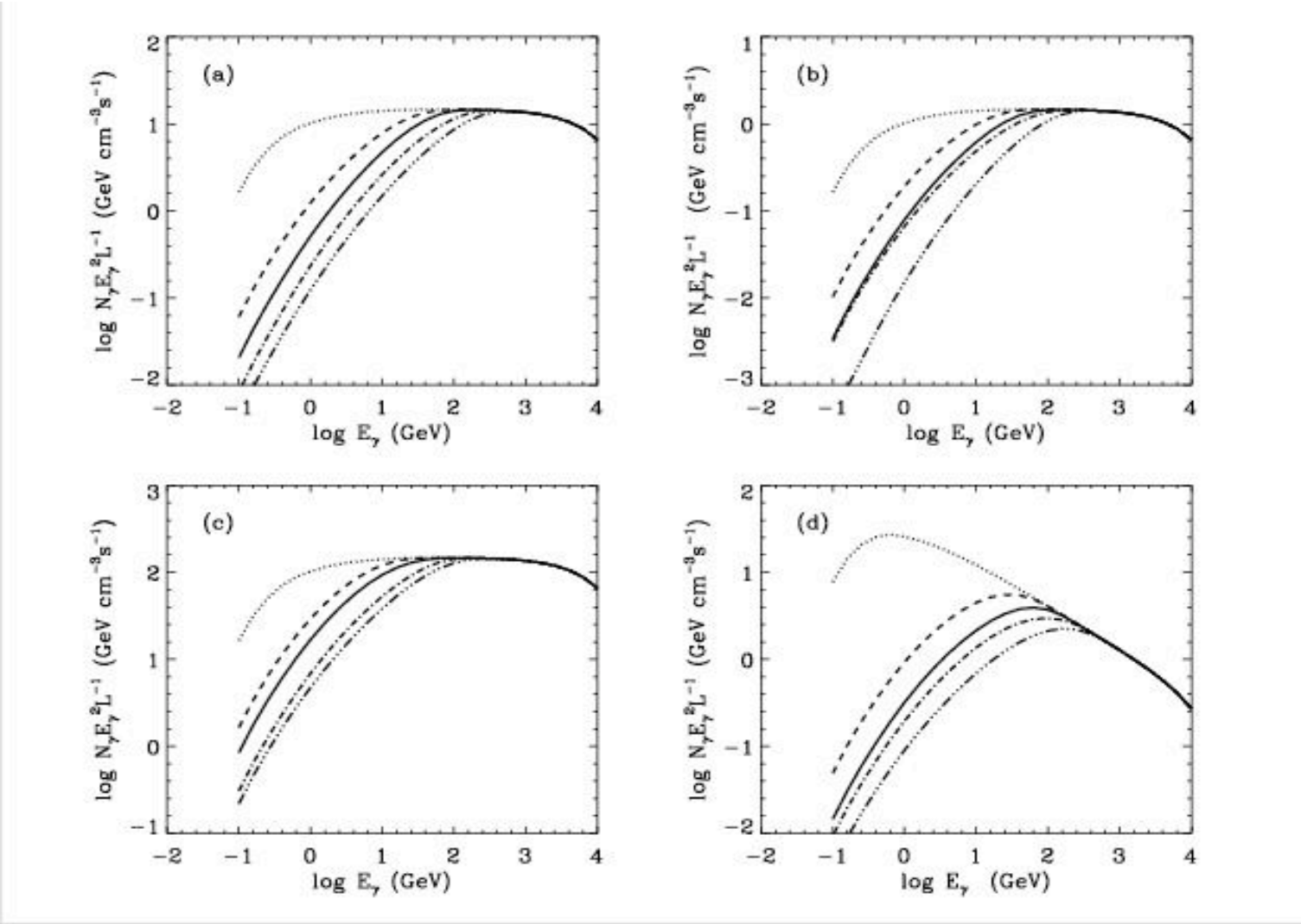

Beall and Bednarek, 1999, 510, 188.

Concluding Remarks:

Plasma processes dominate over other energy loss mechanisms in most cases. In an electron-proton (or electron-hadron) jet, the electrons loose energy to plasma processes more rapidly than do the protons. The jet-protons therefore drag the electrons. This produces a current along the jet in the jet's rest frame. A magnetic field will be generated that could stabilize the jet. This bears further investigation, since it might answer the question of how the jets maintain their coherence for such long distances.

The presence of hadrons in the jet suggest that the jet will produce nuclear gamma-rays and neutrinos as it interacts with the ambient medium (see Beall and Bednarek, Ap.J. 1999). The plasma instabilities modify the emitted gamma-ray spectrum significantly.

We plan to investigate the dynamical consequences of the jet interaction with the intracluster medium using a multiscale approach.

Thanks for your attention